Contest 2015

Title: Southern Lakes Tsunami Hazard

Leader: Dr Joshu Mountjoy
Organisation: NIWA
Total funding (GST ex): $300,000

Updated 10-04-2018

Southern Lakes Tsunami Hazard

Programme Leader: Dr Joshu Mountjoy

Affiliation: National Institute of Water and Atmospheric Research Ltd.

Table of Contents:

Key messages for media 1
Abstract 2
Keywords 2
Introduction 2
Impact Statement 1 4
Research Aim 1.1 4
Research Aim 1.2 6
Research Aim 1.3 7
Research Aim 1.4 11
Research Aim 1.5 15
Conclusions and Recommendations 16
List of End-users 16
List of Outputs 16
References 18
List of Figures 19
List of Tables 19
Acknowledgements 19

Key messages for media

- Tsunamis may be pose a significant hazard to lakeside towns and infrastructure in New Zealand. This pilot study on Lake Tekapo can be used as a basis for research on tsunami hazard in other large New Zealand lakes such as Wakatipu, Wanaka and Taupo.
- Our new data reveal that much of the Lake Tekapo lakebed is affected by landslides, and that individual landslides occur approximately every 1,000 years. There have been at least three regional landslide events that are likely to be earthquake triggered.
- Tsunami modelling indicates that some landslides can generate tsunami waves 5 m above lake level at the southern lake shoreline where the township of Tekapo is located.
- In co-seismic multi-landslide events, the resulting tsunami can be significantly larger, indicating that a large magnitude local earthquake may result in large tsunami in Lake Tekapo.

Abstract

The objective of this research was to develop a method to assess tsunami hazard in lakes. We used Lake Tekapo as a case study to assess the tsunami hazard based on the geological interpretation of source magnitude-frequency relationships and numerical modelling of tsunami scenarios. We have completed mapping and interpretation of landslides on the lake floor and in lake basin sediments. Scenario landslide tsunami models have been developed and the sensitivity of tsunami generation to location and source magnitude assessed.

Landslides occur throughout Lake Tekapo, but the recurrence of events varies for different regions of the lake. Full failure of Cass Delta generates the largest wave heights in the southern half of the lake. Cass Delta has failed multiple times in the past, and our results indicate a recurrence interval of approximately 1,000 years. There is evidence for three concurrent, lake-wide landslide events in the sediment record that are inferred to be co-seismic events. These concurrent events can cause even larger tsunami waves, suggesting that an earthquake which causes significant ground shaking at Lake Tekapo could trigger multiple tsunamis in the lake. Landslides in other regions of the lake also generate significant waves.

Our approach to assess tsunami hazard in lakes can be used as the basis for assessing tsunami hazard in lakes, fiords and harbours worldwide.

Keywords

Landslide Tsunami; Subaqueous Landslide; Lake Tekapo; Tsunami Hazard and Risk

Introduction

This research develops New Zealand's capability to assess the tsunami hazard from terrestrial and subaqueous slope failure in lakes. Large slope failures (also referred to as landslides, mass failures or mass movements) into confined water bodies can produce very large waves in the local vicinity. For example, the largest ever recorded tsunami occurred in Lituya Bay in 1958, resulting from a 30 km^3 terrestrial rock avalanche and creating a wave with a maximum measured runup of over 500 m (Mader & Gittings, 2002). Landslides into and within lakes have also been demonstrated to generate large tsunamis (Kremer et al. 2012). In Italy, on 9 October 1963, a large landslide into the Vajont hydropower reservoir triggered a tsunami that surged up to 250 m high, overtopping the dam and killing 1,925 residents downstream (Kiersch, 1976). These are extreme examples, but they demonstrate the potentially dramatic impact of displacing the relatively small water bodies in lakes, reservoirs and fiords.

Large glacier-formed lakes in the South Island (e.g., Tekapo, Pukaki, Ohau, Wanaka, Hawea, Wakatipu, Te Anau, Manapouri) are surrounded by mountainous terrain and receive high sediment input from glacially-fed rivers. These lakes and valleys are riddled with faults and are all subject to periodic ground-shaking events from regional and local earthquake sources (Stirling et al., 2012), which can cause unstable slopes to fail. Very little is known about the occurrence of slope failures into and within these lakes and the associated tsunami hazard, despite this being identified as a hazard in many studies (Davies, 2007; Clark et al., 2011; Hancox, 2012; Clark et al., 2015). For example, an assessment of the tsunami hazard in Milford Sound determined that large landslides from the steep fiord walls constitute a significant potential threat to visitors and workers in the area; however, wave height estimates were only preliminary, and were calculated by rule-of-thumb methods (Dykstra, 2012).

A 2015 report to Environment Canterbury (Clark et al., 2015) assessed the tsunami hazard in several South Island lakes, and concluded that a significant risk exists, which requires specific work. Report can be found here https://www.ecan.govt.nz/your-region/your-environment/natural-hazards/tsunamis/mackenzie-basin-lake-tsunamis/. Lake Tekapo has been identified as especially vulnerable given its landslide potential and the existence of population and infrastructure at the southern end of the lake. However, a key knowledge deficit is robust information on previous

tsunamigenic sources. By characterising past events, we can determine magnitude-frequency relationships, which will form the basis of the probabilistic hazard assessment.

Little mapping has been carried out on South Island lakes since the 1970’s when lake bathymetry surveying was led by the New Zealand Oceanographic Institute in concert with a major period of hydroelectric power development. Current maps are based on point depths or two-dimensional profiles collected using 40-50-year-old technology. NIWA has new capability to map bathymetry of lakes in high resolution with the latest system designed for a small boat platform (Kongsberg EM2040).

Therefore, the overarching goal of the project was to develop a methodology for efficiently assessing tsunami hazard from landslide sources in New Zealand lakes, building on previous Natural Hazards Research Platform funded work assessing the probabilistic tsunami hazard for landslide tsunami in the Cook Strait Canyons.

The aim was to build a framework for both probabilistic and scenario-based tsunami hazard assessment for confined water bodies using Lake Tekapo as a case study. We achieved this by the following:

- Mapping bathymetry and subsurface sediment structure of the lake to determine the post-glaciation history of slope failure as a basis to quantify source models and magnitude frequency.
- Further developing numerical simulation tools to model tsunami waves generated by a range of terrestrial landslides into lakes and slope failure of sediments within the lakes.
- Modelling specific source scenarios and determining the magnitude frequency for different failure scenarios as a basis for future development of a probabilistic tsunami hazard model to assess the exposure of critical populations and infrastructure.

This report outlines the findings of the research and our conclusions, and is structured around the project’s five Research Aims.

Impact Statement 1

A template for assessing the landslide-tsunami hazard in confined water bodies based on a case study of Lake Tekapo

Research Aim 1.1

Title: Mapping and preliminary data interpretation of Lake Tekapo geomorphology and sediment structure

Research Aim achieved? Yes

Discussion

Desktop study and field planning

Preparations for the field survey, including a desktop study, logistical preparation for fieldwork, field-testing of survey equipment, and specific survey planning and sequencing was carried out between July and December 2015. In addition, following discussions with researchers at Otago University also interested in Lake Tekapo, we coordinated an approach to acquire higher resolution Chirp Seismic and sediment cores using University of Otago vessel and equipment.

Field work methods

The acquisition of multibeam bathymetry and seismic reflection data took place during the first two weeks of February 2016. Figure 1A shows the coverage of acquired data. We collected ~80 km^2 high resolution lake bathymetry using a Kongsberg 0.4 x 0.7 degree EM2040 echo-sounder. The system was deployed from a 6.8 m monohull vessel with a customised pivoting bow-mounted deployment system to lower the EM2040 pod into the water (Wilcox et al., 2016). This system allows the pod to be deployed easily once onsite with a high degree of repeatability. Position and attitude information is provided by an Applanix POSMV system with the antenna mounted directly above the EM2040 pod. Data were acquired using SIS data acquisition system and processed in Caris HIPS. Data covered the entire lakebed up to approximately the 10 m bathymetry contour. Shallower than this was considered both too risky for navigation as there are no navigation charts available for this lake, and too time consuming as the swath width becomes narrow in shallow water depth.

We also collected 130 km of 2D multi-channel boomer seismic data and 54 km chirp seismic data (Figure 1). The seismic acquisition system consisted of a 200 kJ boomer source and a 16-channel GeoEel digital seismic streamer (Geometrics) with a hydrophone group spacing of 1.562 m. Both were towed approximately 20 m behind the monohull vessel with 3 m perpendicular offset between source and streamer, and 10.8 m offset from source to first channel. Data were acquired with a shot rate of 1-2 Hz and a recording length of 400 or 500 ms with navigation strings provided by the POSMV system written to the seismic data header. Standard seismic data processing with a special deconvolution to suppress ringing in the data was undertaken using Globe Claritas®. A remaining seafloor multiple artefact could not be eliminated with post processing. The overall quality of the data is good, showing penetration of up to 300 m and a vertical resolution of 0.4 m. Chirp data were acquired using a Knudsen Pinger 3.5 kHz sub-bottom profiler deployed on an over-the-side mount from an inflatable craft. The inflatable was towed 30 m behind a monohull power boat at 3 knots. Towing the chirp at low speeds ensured an excellent signal-to-noise ratio and data quality. Positional information for each ping was acquired using a handheld Garman csX60 GPS unit with an accuracy of ±4 m. All data were loaded into a Kingdom Suite® project for interpretation.

Bathymetric and seismic data have been interpreted to map out surface features in bathymetric data such as landslide scars and deposits, sediment deltas and sediment waves (Figure 1), and subsurface features in seismic, data including depth to basement, landslide deposits and regional horizons. This work is presented in Mountjoy et al. (In press 2018). These interpretations are used to guide the project's other Research Aims.

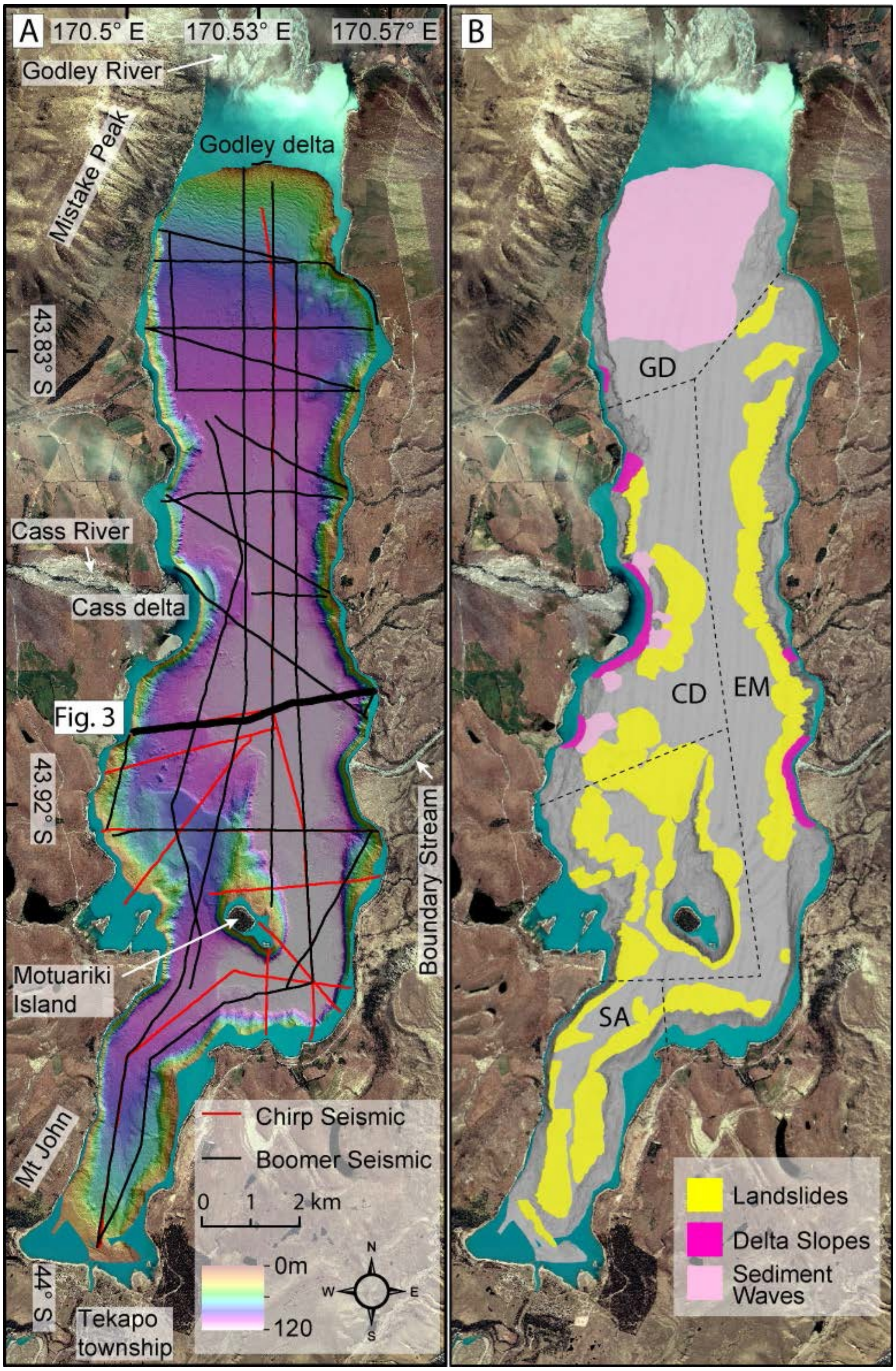

Figure 1: Lake Tekapo mapping. A) Physiographic features around Lake Tekapo and data collected for this project. Areas of coloured shading in the lake show the bathymetric mapping extent with areas around the lake margin in blue (also in Panel-B) unable to be mapped due to shallow water depths. B) mapped surface features in the lake related to sediment movement. Scale is the same as for Panel-A. Dashed lines indicate different landslide zones in the lake, GD Godley Delta, CD Cass Delta, EM Eastern Margin, SA South Arm. The un-named area between SA and CD is a region of undifferentiated landslide deposits. Figure modified from Mountjoy et al. (In press 2018).

Research Aim 1.2

Title: Model development for simulating both landslide and subsequent tsunami in confined water bodies

Research Aim achieved? Yes

Discussion

Model Development

Landslide-induced waves in confined waters such as lakes, fjords and reservoirs affect the area close to the tsunami source and the waves tend to be more dispersive. Approaches for submarine landslide tsunami modelling developed for oceanic settings may not be suitable for enclosed water bodies, and new techniques are required. The requirements include the development of modelling capabilities of landslide motions on relatively steep slopes with terrestrial-to-subaqueous transition, dynamical generation and evolution of dispersive waves by landslide motions, and coastal flooding especially in the vicinity of landslide sources.

In partnership with GNS UET-funded research and a National Natural Science Foundation of China funded project, we have further developed a fully coupled two-layer landslide-tsunami joint simulation model in the widely used COMCOT tsunami package (Wang & Power 2011). This model was originally created for non-dispersive to weakly dispersive submarine landslide tsunamis. It simultaneously calculates the evolution of subaerial/subaquatic landslides as either solid-block motions or avalanches for the dynamic generation of tsunami (Wang et al. 2016). With the new developments, the model also includes the dynamic generation process of tsunami waves, tsunami propagation, and coastal flooding using wave models based on multi-layer Boussinesq-type depth-integrated equations for a greatly improved dispersion relationship. A robust moving boundary scheme was also developed to model the potential lake shore flooding in the area where the sliding mass enters the water. The development of this dynamically coupled landslide-tsunami joint simulation model not only overcomes the weakness of traditional static initial condition approaches for submarine landslide tsunami modelling, but also provides the capability of realistically evaluating coastal flooding in the near vicinity of where a landslide enters a water body.

Model Applications

This landslide-tsunami joint simulation model was used to evaluate tsunami hazards by subaerial, subaqueous landslides, and simultaneous failure of multiple landslides in Lake Tekapo as reported on in RA 1.3. It has also been successfully applied to simulate potential failures of Guopu slope in the Laxiwa Reservoir in China to evaluate the resulting surge wave impacts under different impoundment conditions.

Research Aim 1.3

Title: Landslide tsunami scenario modelling

Research Aim achieved? Yes

Discussion

To carry out numerical landslide tsunami simulations, we developed a seamless Digital Elevation Model (DEM) of Lake Tekapo lake floor and the immediate surrounding area. The high-resolution DEM was developed at an interpolated grid spacing of 5m by combining the multi-beam bathymetric survey data, New Zealand 8 m DEM (LINZ 2012) and the 1973 Chart contours of Lake Tekapo. The model grid uses the lake level at the time (710 m asl) as the datum water level (https://www.genesisenergy.co.nz/tekapo-lake-level) and New Zealand Transverse Mercator 2000 projection for the development of this DEM dataset.

Scenario Modelling

Several landslide scenarios were modelled based on the interpretations of landslide location, size and kinematics from newly acquired data (RA 1.1) to assess the relative hazard posed by failures at different locations around the lake (Table 1 and Figure 2). We did not model scenarios related to the failure of Mount John as we did not observe any clear evidence for deposits related to slope failure there despite the relatively good seismic imaging beneath the slope. We did, however, model three terrestrial failure scenarios (S07-S09) coming from Mistake Peak (Figure 1), which rises approximately 1,000 m above the lake shore. Scenarios V01 and V02 as shown in Table 1 and Figure 2 were used to validate the landslide model parameters based on the observed runout. Details of the validation and modelling code are provided in Mountjoy et al. (In press 2018). We then used these parameters to simulate the failure process of the other landslides, and subsequently modelled the dynamic generation of tsunamis, tsunami propagation and inundation.

Table 1: Summary of modelled landslide scenarios. For the failure types, subaqueous failures are wholly within the lake, lake margin failures have failed part of the shoreline as well, and terrestrial failures are wholly sourced on land. Mixed failures are a combination of these.

Scenario	Location (Figure 1)	Failure Type	Volume (km3)
Scenario 01 (S01)	Southern Arm	Subaqueous	0.0015 km^3
Scenario 02 (S02)	Eastern Margin	Subaqueous	0.0135 km^3
Scenario 04 (S04)	Cass Delta	Lake margin	0.0085 km^3
Scenario 05 (S05)	Cass Delta	Lake margin	0.0930 km^3
Scenario 06 (S06)	Godley Delta	Lake margin	0.0281 km^3
Scenario 07 (S07)	Mistake Peak	Terrestrial failure	0.0016 km^3
Scenario 08 (S08)	Mistake Peak	Terrestrial failure	0.0097 km^3
Scenario 09 (S09)	Mistake Peak	Terrestrial failure	0.0021 km^3
Validation 01 (V01)	Eastern Margin	Lake margin	0.0336 km^3
Validation 02 (V02)	Cass Delta	Lake margin	0.0093 km^3
S01_0010km3	Southern Arm	Subaqueous	0.0010 km^3
S01_0020km3	Southern Arm	Subaqueous	0.0020 km^3
Concurrent C00	V01+V02	Lake margin	0.0429 km^3
Concurrent C01	S01+S05+S06	Mixed	0.1226 km^3
Concurrent C02	C01+S02+S04+S08+V01	Mixed	0.1501 km^3

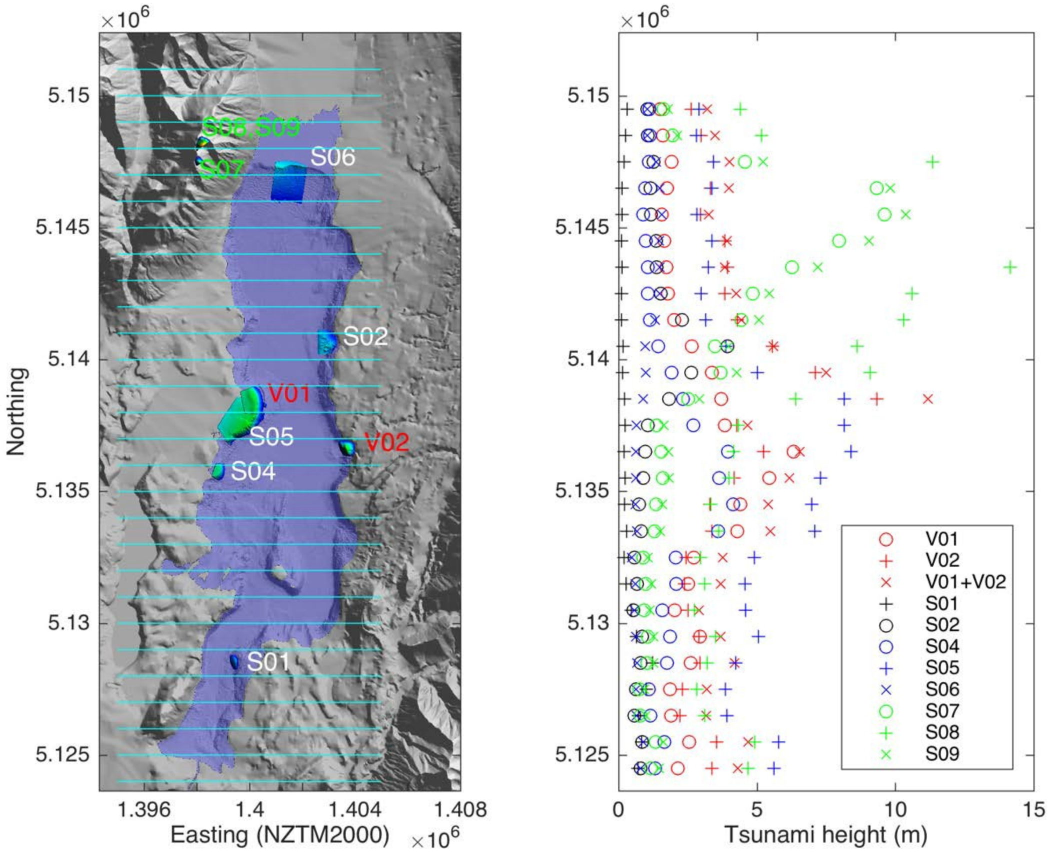

Figure 2: Tsunami modelling results from individual landslide scenarios. Left Panel: Location of scenario sources. Blue horizontal lines indicate the division of aggregated tsunami heights presented in right hand panel. Right Panel: Maximum tsunami height at lake shore in metres above lake level for each tsunami source modelled. Tsunami height shown in the right panel is an average of maximum tsunami heights at coasts within 1km wide horizontal strips separated by blue lines in the left panel. After Mountjoy et al. (In press 2018)

The modelling of scenario S05 is detailed here as an example to illustrate the approach of landslide tsunami simulations that has been applied to all the scenarios. The left panel of Figure 3 shows the initial thickness distribution of landslide mass failure at Cass Delta in scenario S05, with an estimated volume of about 0.093 km^3. It is the largest among all the individual failure scenarios. Together with the high-resolution DEM data, this initial thickness data was used as input to the coupled landslide-tsunami joint simulation model to simulate the failure process of the landslide mass and resulting tsunami in Lake Tekapo for a period of three hours after the landslide to obtain the maximum tsunami heights above lake level throughout the lake, including potential inundation of land surrounding the lake. The right panel of Figure 3 illustrates the spatial distribution of the modelled maximum tsunami heights of landslide scenario S05 in Lake Tekapo. Maximum wave heights occur at the shoreline opposite the source and results in tsunami heights over 5 m at the southern shoreline.

The results of all the modelled scenarios show water levels over 5 m above lake level are present in many locations but predominantly in the immediate vicinity of the source area. Sub-aqueous landslides in the northern region of the lake (e.g., SO2, SO6) generate only modest wave heights at the southern shore of the lake. Terrestrial landslides initiating on the flank of Mistake Peak (SO7, SO8 and S09) generate waves with peak water levels >10 m where they enter the lake but these attenuate to the south over a short distance (Figure 2). In scenario SO8 however, shoreline water levels are still approximately 5 m at the southern end of the lake near Tekapo Township.

To assess the influence that multiple concurrent failures have on tsunami generation we also modelled a number of simultaneous slope failures, e.g., concurrent failure scenarios C01 and C02 in Table 1. The results from concurrent failures C00 in Table 1 are shown in Figure 2. Concurrent

scenarios result in significantly enhanced wave heights around the lake (Figure 4) and indicate that multiple slope failures triggered by a local earthquake may pose the most significant tsunami hazard in Lake Tekapo.

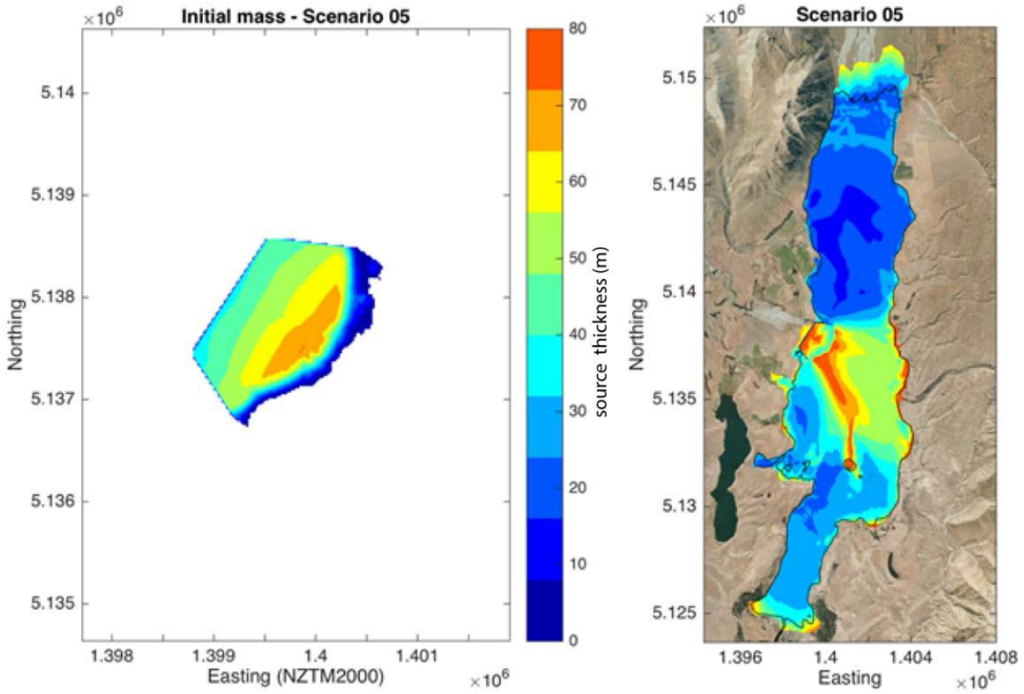

Figure 3: Tsunami modelling for Scenario S05. Left Panel: Spatial thickness distribution of the initial state of the mass failure for landslide scenario S05 – Cass Delta failure. Right Panel: Spatial distribution of the modelled maximum tsunami height in Lake Tekapo for landslide scenario S05.

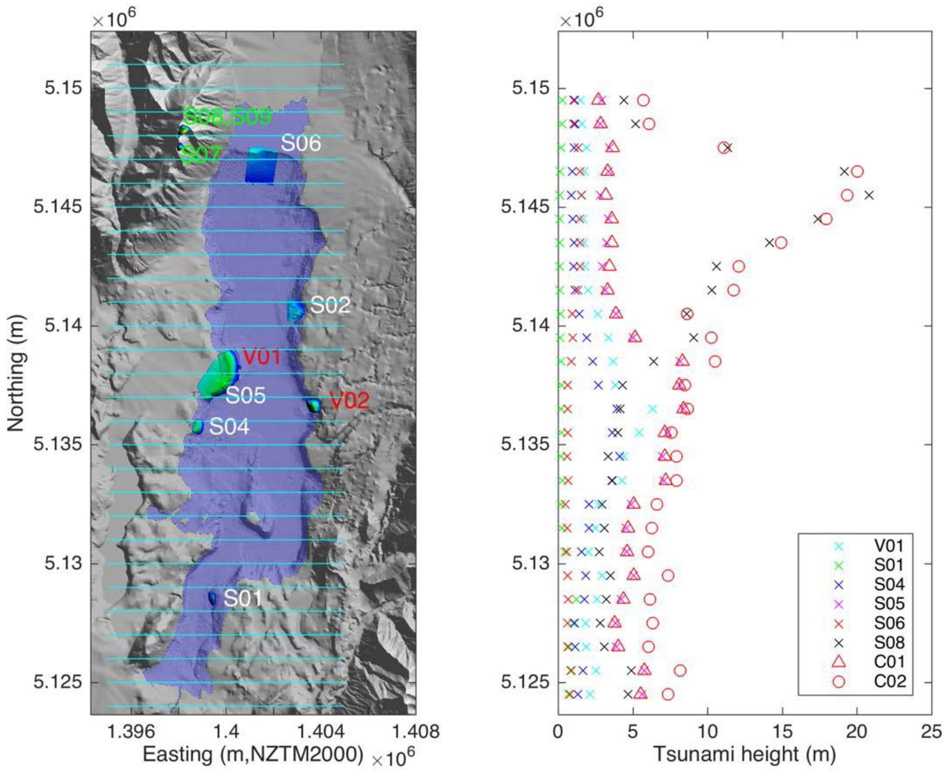

Figure 4: Spatial distribution of modelled maximum tsunami heights in Lake Tekapo for concurrent failures C01, C02 and their individual failure scenarios. Left panel shows failure location and aggregated result regions defined by blue lines. Right panel shows average of maximum tsunami heights in metres above lake level within 1 km wide horizontal strip as illustrated in the left panel.

Close examination of these concurrent failure scenarios also reveals the effect of interactions among tsunami waves triggered by individual landslide sources in a concurrent failure scenario. For example, the maximum tsunami height of a concurrent failure is not always larger than those of its individual scenarios, even smaller at a few locations, presumably due to destructive interference of waves (Figure 5). This implies that timing between individual landslide failures is an important factor in the evaluation of tsunami hazard in multiple failure scenarios. This phenomenon will need to be subject to further investigations.

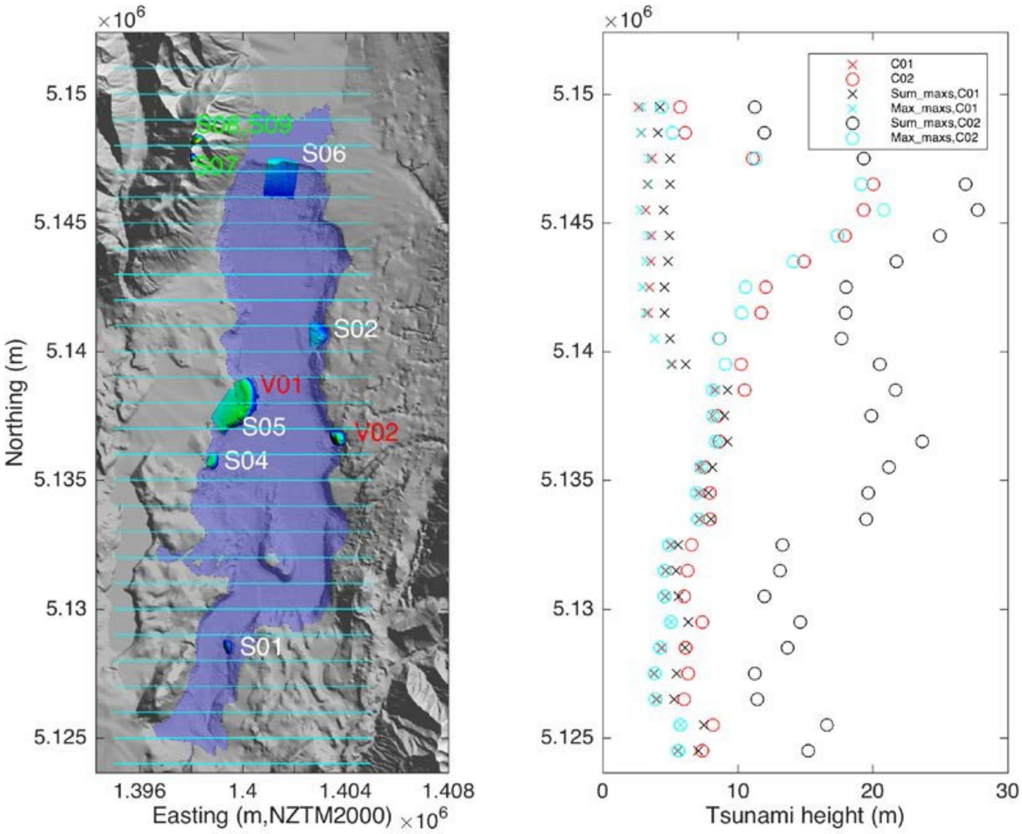

Figure 5: Spatial distribution of modelled maximum tsunami heights along the coasts of Lake Tekapo for concurrent failures C01, C02 and their individual failure scenarios. Left panel shows failure location and aggregated result regions defined by blue lines. Right panel shows average of maximum tsunami heights in metres above lake level within 1 km wide horizontal strip as illustrated in the left panel. In the legend, Sum_maxs denotes the sum of all the individually modelled maximum tsunami heights of the failure scenarios included in the concurrent failure; and Max_maxs means the maximum of all the individually modelled maximum tsunami heights of the failure scenarios included in the concurrent failure.

Research Aim 1.4

Title: Development of a landslide magnitude frequency relationship

Research Aim achieved? Yes

Discussion

The post-glacial sediment fill in the lake provides an approximately 12,000-year record of landslide occurrence based on glacial retreat timing (Shulmeister et al., 2010) and extrapolation of accumulation rates. The possible range is between 10,000–15,000 years. We use this estimated record length to determine slope failure magnitude-frequency relationships. Bathymetry and seismic data show that different regions of the lake basin experience different failure modes and recurrence intervals. Figure 6 shows an example of repeated slope failure deposits through the lake basin, including concurrent failure in the upper part of the sequence. Seismic horizon ages are defined using existing accumulation rate data (Graham et al., 2005; Mildenhall et al., 2006). The age data derived from cores collected in conjunction with this project are still being processed. These horizon ages constrain the timing of landslide events and are used to define mean recurrence periods for slope failure within the different zones indicated in Figure 1B.

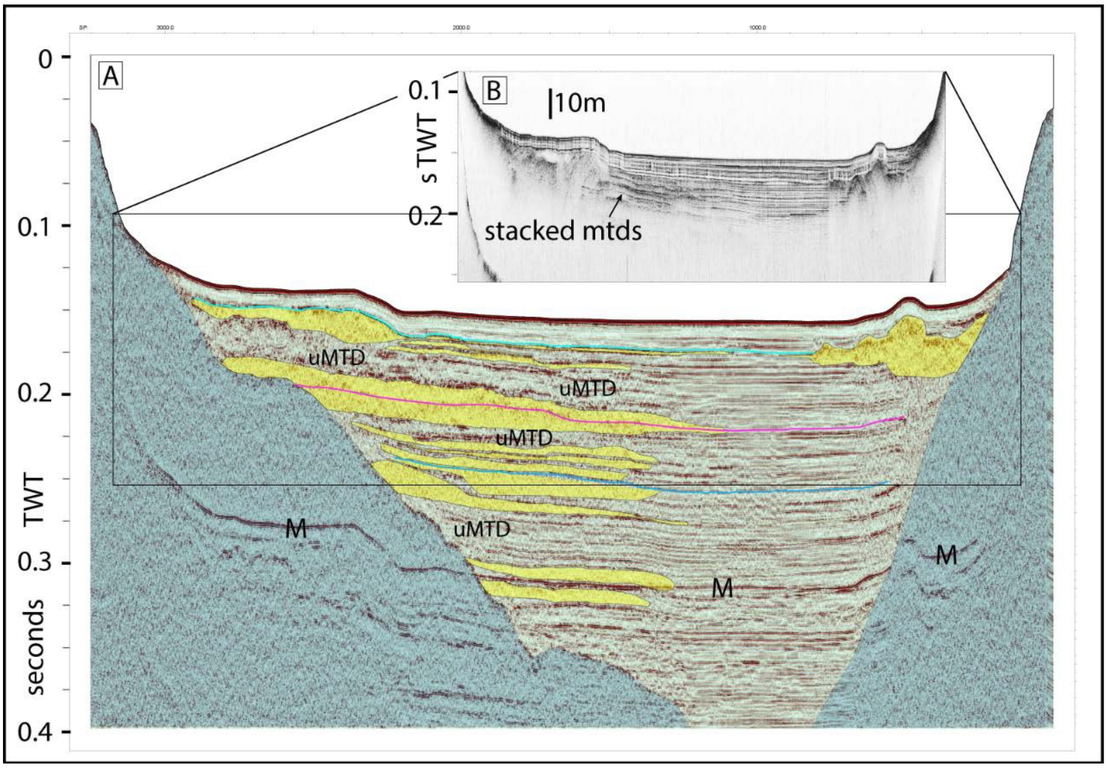

Figure 6: Seismic profile illustrating MTDs in the central lake basin and three key regional horizons. uMTD indicates undifferentiated MTDs. M indicates lake floor multiple. Zoom panel at top is 3.5 kHz chirp data collected at the same location. Profile location in Figure 1. After Mountjoy et al. (In press 2018).

Cass Delta

Tsunami modelling has shown the Cass Delta (Figure 1) to be the source location of the main tsunami hazard affecting the Tekapo township. A sequence of 11 landslide deposits were found at the Cass Delta, interpreted to be a complete record of large landslides (deposit volume > $4.3*10^6$ m^3) from this delta since the last glaciation (Table 2). From this dataset, a magnitude frequency relationship can be derived, although there are large uncertainties involved. Of these 11 landslides, 3 are interpreted to occur at the same time as multiple lake-wide landsliding events, and 8 interpreted to be independent events in which the Cass Delta is taken to be the only or predominant landslide event.

Table 2: MTDs recognised in seismic and correlated with the failure of Cass Delta.

Landslide-ID	Deposit volume V_d (m^3)
MTD-X1	9,757,440
MTD-X2	9,757,440
MTD-X4	27,256,320
MTD-X4.1	40,824,000
MTD-X4.5	6,445,958
MTD-X4.6	4,354,560
MTD-X5	5,110,560
MTD-X6	14,062,066
MTD-X7	16,100,332
MTD-X8	9,686,880
MTD-X9	10,596,600

If we first consider landsliding of the whole set of Cass Delta failures, then an estimate of the annual probability can be obtained by dividing the number of failures by the number of years since glaciation. It is important to note here that this analysis assumes that such a failure is equally likely to occur at any time, whereas these failures are likely to be cyclic (a certain length of time is required for the delta to rebuild between collapses) and therefore the annual probabilities are likely to increase with time since the last collapse.

Given that a failure has occurred, an estimate can be made of the likelihood of exceeding a specific volume, by curve-fitting to the cumulative distribution of events (Figure 7).

Table 3: Probability results for failure of Cass Delta

Scenario	Annual probability
All Cass Delta failures	11/12,000 ≈1/1,090 ≈ 0.00092
Cass Delta failures not part of lake-wide failures	8/12,000 ≈ 1/1,375 ≈ 0.00073
Cass Delta failures part of lake-wide failures	3/12,000 ≈ 1/3,367 ≈ 0.00027

From the cumulative distribution in Figure 7 we arrive at the empirical relationship, that in the event of a large (deposit > $4.3*10^6$ m^3) landslide the probability whose deposit exceeds a volume V_d is given by:

$$Pr(\text{deposit exceeds volume } V_d) = -0.431 \ln(V_d) + 7.5478$$

Only part of the original failure volume is found in the final deposit, we assume that approximately half of the original failure material becomes sediment that is widely distributed across the lake: V_f = $2V_d$. Hence:

$$Pr(\text{mass failure exceeds volume } V_f) = -0.431 \ln(V_f/2) + 7.5478.$$

For the purpose of generating synthetic catalogues for use in hazard and risk analysis, it is convenient to rearrange this equation:

$$V_f = 2 * \exp\left((7.5478 - R) / 0.431\right).$$

Where R is a uniformly distributed random variable.

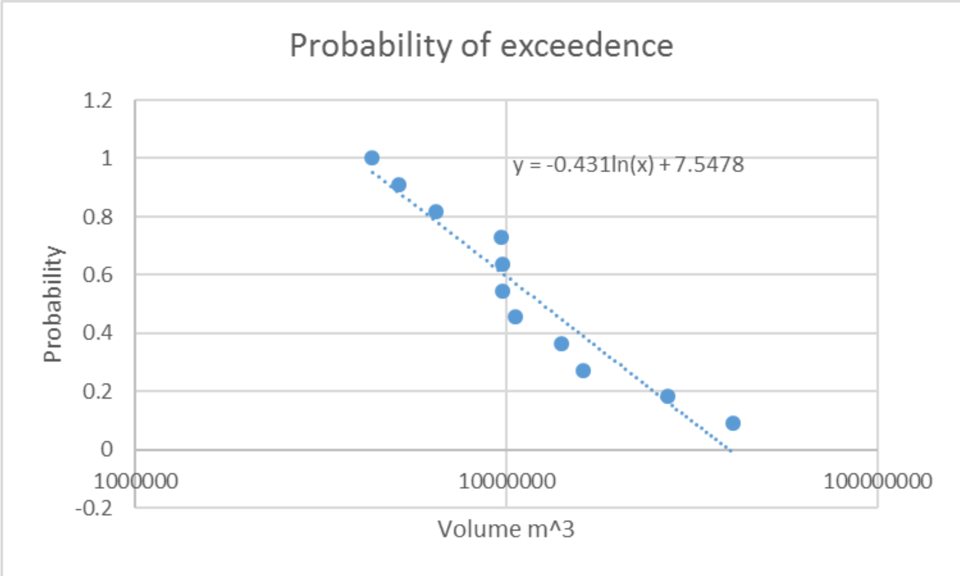

Figure 7: Conditional probability of landslide deposit volume exceedance for Cass Delta mass failures exceeding $4.3*10^6$ m^3. Solid points represent individual landslide data points (from Table 3). The dashed line shows a logarithmic curve fit.

For the case of all Cass Delta failures (i.e., making no distinction between those that correlate with lake-wide failures and those that do not), the combination of the annual probability of failure with the conditional probability of a given volume, leads to the recurrence relationship shown in (Figure 8).

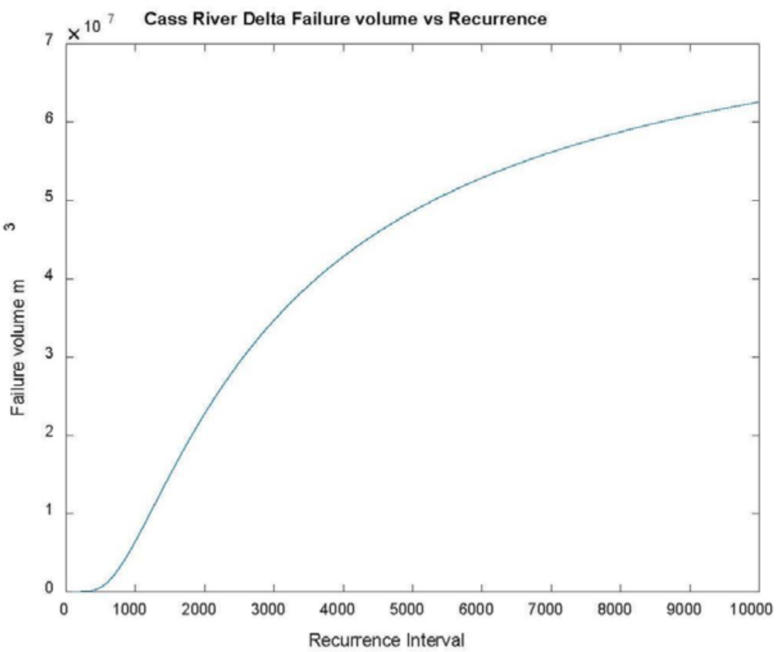

Figure 8: Magnitude-frequency relationship for failures of the Cass Delta, showing the expected failure volume as a function of recurrence interval. See text for derivation. The curve is poorly defined for recurrence intervals of less than 1000 years.

Southern Lake Arm

A total of $25*10^6$ m^3 of landslide debris has accumulated in the Southern Arm (Figure 1) over a period estimated to be 4,000 years based on correlation of seismic horizons from the main lake basin. This period encompasses two of the events in which there was widespread landsliding around the lake. We assume that failures similar to S01 ($1.5*10^6$ m^3) are typical of failures in this arm, and that half of the accumulated $25*10^6$ m^3 of landslide debris occurred during the two events in

which there was multiple landslides. This would suggest that in the 4,000-year period there were approximately 25 / 1.5 = 17 landslides (if all were similar in volume to S01), of which about half occurred at the same time as the lake-wide landsliding events.

An estimate of the annual probability for landslide occurrence in the Southern Arm, that occur separate from the multiple landslide events, is 8.5 / 4000 ≈ 0.0021 ≈ 1/471. Indicating discrete events have a recurrence interval of approximately 471 years. This is an approximation as it does not allow for variation in the landslide volume, and the assumption about the proportion of debris that occurred during multiple landslide events is unconstrained. Past landslides in the Southern Arm appear to be widely spatially distributed around the lake perimeter.

Regional events involving multiple failures lake-wide

Evidence for three multi-landslide events has been identified. Based on our estimated age of the basin fill sequence, we estimate an annual probability of 4/12,000 ≈ 1/3,000, or an average recurrence interval of 3,000 years. All of the region-wide events appear to include both Cass Delta and Godley Delta failures.

Godley Delta

Evidence for three episodes of failures in the Godley Delta (Figure 1) have been identified. Based on our estimated age of the basin fill sequence we derive an annual probability of 4/12,000 ≈ 1/3,000, or an average recurrence interval of 3,000 years. However, all of these failures were contemporaneous with the regional events that involved multiple lake-wide failures.

Research Aim 1.5

Title: Probabilistic modelling of tsunami hazard from discrete source areas in confined water bodies

Research Aim achieved? Partial

Discussion

A technique for estimating tsunami hazard from discrete sources in confined water bodies was developed and implemented in Matlab. The method uses a synthetic catalogue approach and is flexible regarding the number of potential tsunami sources. For each source, three inputs are required— (1) A recurrence interval for events of the particular type; (2) A conditional probability function for the landslide to exceed a given volume; and (3) A relationship, derived through modelling and curve fitting, between the landslide volume and the tsunami height at the site of interest. Figure 9 shows an example of a tsunami hazard curve that was developed using 'dummy' data consisting of three different landslide sources.

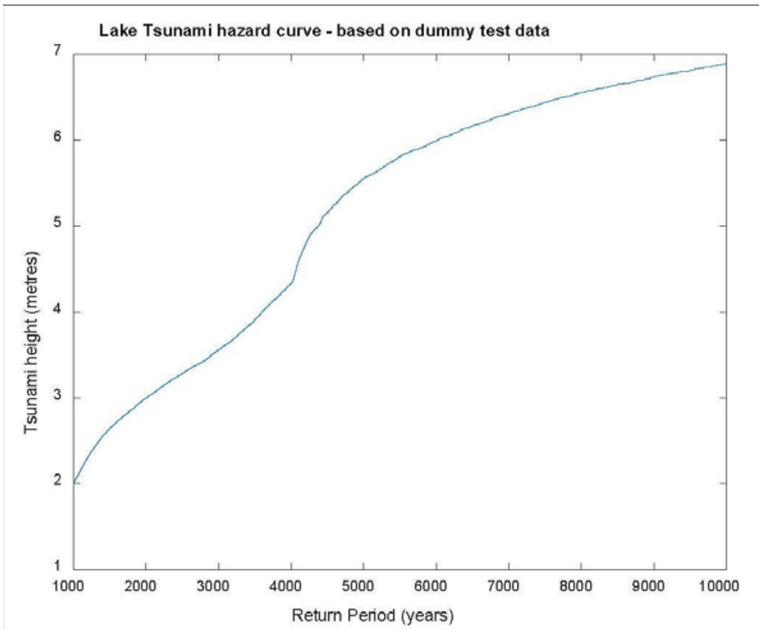

Figure 9: An example of an estimated tsunami hazard curve, showing expected lake-shore tsunami height in metres as a function of return period in years. This figure was generated using artificial 'dummy' input data

Not all inputs needed to apply the probabilistic model to Lake Tekapo could be quantified, so it was not possible to produce a tsunami hazard curve for this site. This is partly because we didn't anticipate the importance of basin-wide events involving multiple landslides from sources all around the lake. Resources from this Research Aim were diverted to better understand the potential impact of such events (see RA 1.3). A justifiable approach to quantifying the potential tsunami heights at the Lake Tekapo township in the probabilistic model requires further research, as the tsunami height is likely to be a function of the set of different landslides involved, which cannot be anticipated in advance, and may also be sensitive to the precise timing of the landslides. Another limitation in developing the probabilistic model is that landslides originating on Mistake Peak could be a source of some of the largest tsunami waves to reach Tekapo township; however, the presence of sub-surface gas in the northern end of the lake has made it impossible to estimate the volume or frequency of past events of this type. Consequently, there is a gap in the data needed to form a magnitude-frequency relationship for this source. This problem may be addressed either by drilling through the sediment layers in this part of the lake, or by geotechnical analysis of the slopes of Mistake Peak. The framework we have developed in intended to underpin a future probabilistic model to assess the exposure of the township and hydropower infrastructure adjacent to Lake Tekapo.

Conclusions and Recommendations:

This research was the first comprehensive approach taken to assessing landslide tsunami in a New Zealand lake. We used Lake Tekapo as our case study as it has an identified potential tsunami hazard, mid-range water depth and size for ease of surveying, and population and infrastructure exposed to inundation.

We mapped the lake floor and subsurface, revealing widespread sediment mass failure. Seismic stratigraphy indicate that the most recent phase of large-scale landsliding occurred concurrently at many locations around the lake, indicating an earthquake trigger. The record indicates three concurrent failure events since glacial retreat approximately 12,000 years ago. Different regions of the lake have distinctly different histories of mass failure. Recurrent failure has occurred from Cass Delta on the western shore, suggesting that this is likely to be an area that will fail in the future.

We advanced the development of numerical modelling code for a coupled simulation of lake floor mass-failure and tsunami, and used this new code to assess the tsunami-generating potential of individual scenario landslides, as well as multiple concurrent landslides. We also used the magnitude- frequency relationships developed for different zones in the lake to develop the framework for a probabilistic tsunami model.

Tsunami modelling results show that landslides of the size observed in the geological record can generate significant tsunami in the lake and at the southern shore. When multiple scenarios are simulated concurrently, tsunami heights may be significantly increased. This indicates that an earthquake capable of basin-wide landslide triggering poses the most significant tsunami hazard. Full failure of the Cass Delta alone has the potential to generate waves over 5 m above lake level at the southern shore of the lake.

Although inundation modelling was included in the model output (e.g., Figure 3) the uncertainty associated with any absolute values are high, as our digital elevation model did not include high resolution mapping of the very shallow water or shoreline (e.g., LiDAR). We recommend that inundation modelling should be undertaken, given the magnitude of the modelled tsunami, to determine the risk posed to the township of Tekapo, infrastructure and periodically highly populated tourist destinations. To provide a complete and robust result, the probabilistic modelling should be implemented, which requires further information on terrestrial source tsunami potential at the northern end of the lake. Based on this study, the highest hazard for Tekapo Township is associated with failure of Cass Delta and a focused stability assessment of this is recommended.

List of End-users

The project had five key end-users. McKenzie District Council, Environment Canterbury Regional Council, Genesis Energy Limited, the Ministry of Civil Defence and Emergency Management, and the New Zealand science research community

List of Outputs

Peer-reviewed Journal publications

Mountjoy, J. J., X. Wang, S. Woelz, S. Fitzsimons, J. D. Howarth, A. Orpin and W. L. Power (in press 2018). "Tsunami hazard from lacustrine mass wasting in Lake Tekapo, New Zealand." Geological Society of London Special Publications Subaqueous Mass Movements and Their Consequences: Assessing Geohazards, Environmental Implications and Economic Significance of Subaqueous Landslides. (GSLSpecPub17-225R1).

Liu, Y., X. Wang, Z., WU, Z., HE and Q., YANG (Submitted). Simulation of landslide- induced surges and analysis of impact on dam based on stability evaluation of reservoir bank slope. Revised version in review at Landslides.

Industry articles

Wilcox, S., P. Notman and J. Mountjoy. (2016). "Lake Tekapo Survey." from https://www.km.kongsberg.com/ks/web/nokbg0238.nsf/AllWeb/E1B5A1B958E8D783C1257F87002E3826?OpenDocument.

Conference presentations

S.Woelz, J. Mountjoy, A. Orpin, S. Wilcox, P. Gerring, S. Fitzsimons, J. Howarth, and C. Mueller. (2016). New Seismic and Acoustic Insights into Lake Tekapo. In: Riesselman, C. and Roben, A.(eds). Abstracts, Geosciences 2016, Wanaka, Geoscience Society of New Zealand Miscellaneous Publication 145A. p.99

Two presentations for the Geosciences 2016 conference in Wanaka on the Lake Tekapo project were submitted but were not presented due to demands of the November 2016 Kaikoura Earthquake.

Wang, X., W. Power, J. Mountjoy and Y. Liu. "Evaluating wave impact by slope failures in confined water bodies with a coupled landslide-tsunami model" KOZWAVES 2018. 12 to 14 February 2018. Auckland New Zealand.

Mountjoy, J. J., X. Wang, S. Woelz, S. Fitzsimons, J. D. Howarth, A. Orpin and W. L. Power (Accepted). "Tsunami hazard from lacustrine mass wasting in Lake Tekapo, New Zealand." VIII International Symposium on Submarine Mass Movements and Their Consequences. 7-9 May 2018. Victoria, Canada.

Liu, Y., X. Wang, Z. Wu, Q. Yang, J. Mountjoy and W. Power (accepted). "A joint assessment framework for bank slope stability, slope failure and landslide tsunami hazard in reservoirs, lakes and fjords" AOGS 15th Annual Meeting. 03 to 08 June 2018. Honolulu, Hawaii.

Wang, X., W. Power, J. Mountjoy and Y. Liu. (accepted). "Evaluation of terrestrial and subaqueous landslide tsunami hazard in Lake Tekapo, New Zealand" AOGS 15th Annual Meeting. 03 to 08 June 2018. Honolulu, Hawaii.

Workshops

Power, W. Presentation on 'Lake Tsunamis' to the National Health Emergency Managers Forum in Wellington on the 2 November 2017.

Power, W. Participation in scenario exercise for the forum participants simulating the response to a large Alpine Fault earthquake.

Mountjoy, J., Power, W. Presentation to McKenzie District Council; Environment Canterbury and the Tekapo Community Board. This meeting was delayed due the 2016 Kaikōura Earthquake and has been rescheduled for early 2018

Mountjoy, J., Power, W. Open presentation to the Tekapo Community. *This meeting was delayed due the 2016 Kaikōura Earthquake and has been rescheduled for early 2018*

Media

http://www.stuff.co.nz/science/78016300/More-than-half-of-Tekapo-lake-bed-covered-in-large-landslides

https://www.radionz.co.nz/news/regional/299324/landslide-finds-prompt-tsunami-fears

https://www.niwa.co.nz/news/niwa-completes-first-bathymetric-mapping-of-lake-tekapo

https://www.tvnz.co.nz/one-news/new-zealand/lake-tekapo-chosen-probe-risk-tsunamis-new-zealand-lakes

References

Clark KJ, Hancox GT, Forsyth PJ, Pondard N, Power W, Strong D, Lukovic B 2011. Identification of Potential Tsunami and Seiche Sources, Their Size and Distribution on Lakes Te Anau and Manapouri. GNS Science Consultancy Report 2011/196 p.

Clark KJ, Upton P, Carey J, Rosser B, Strong D 2015. Tsunami and Seiche Hazard scoping study for Lakes Tekapo, Pukaki, Ohau, Alexandrina and Ruataniwha. *GNS Science Consultancy Report* 2014/227 82 p.

Davies TW 2007. Natural event and human consequences in Queenstown Lakes and Central Otago. http://www.orc.govt.nz/Information-and-Services/Natural-Hazards/Great-Alpine-Fault-Earthquake/

Dykstra JL. 2012. The Post-LGM Evolution of Milford Sound, Fiordland, New Zealand: Timing of Ice Retreat, the Role of Mass Wasting & Implications for Hazards. Thesis. University of Canterbury.

Graham I, Alloway B, Cochran U, Cook R, Ditchburn R, Mildenhall D, Morgenstern U, Prior C 2005. Sedimentology, geochronology and micropaleontology of post-and immediately pre-European Lake Tekapo sediment (based on analysis of core L1395). Institute of Geological & Nuclear Sciences science report 2005/34 82p p.

Hancox GT 2012. Environment Southland Tsunami and Seiche Study - Stage 2: Evaluation of Potential Earthquake-Induced Landslide Sites Where Tsunami Waves Could Be Generated on Lake Manapouri and Lake Te Anau. GNS Science Consultancy Report 2012/146 p.

Kiersch GA 1976. Vaiont reservoir disaster. Focus on Environmental Geology. R. Tank, ed

Kremer K, Simpson G, Girardclos S 2012. Giant Lake Geneva tsunami in AD 563.

Nature Geosci 5: 756-757.

Mader CL, Gittings ML 2002. Modeling the 1958 Lituya Bay mega-tsunami, II. Science of Tsunami Hazards 20: 241-250.

Mildenhall D, Cochran U, Cook R 2006. Reconnaissance sediment and microfossil analyses of a laminated short piston core from Lake Tekapo, South Island, New Zealand. New Zealand Journal of Geology and Geophysics 49: 463-476.

Mountjoy JJ, Wang X, Woelz S, Fitzsimons S, Howarth JD, Orpin A, Power WL In press 2018. Tsunami hazard from lacustrine mass wasting in Lake Tekapo, New Zealand. Geological Society of London Special Publications Subaqueous Mass Movements and Their Consequences: Assessing Geohazards, Environmental Implications and Economic Significance of Subaqueous Landslides.:

Shulmeister J, Fink D, Hyatt OM, Thackray GD, Rother H 2010. Cosmogenic 10Be and 26Al exposure ages of moraines in the Rakaia Valley, New Zealand and the nature of the last termination in New Zealand glacial systems. Earth and Planetary Science Letters 297: 558-566.

Stirling Met al. 2012. National Seismic Hazard Model for New Zealand: 2010 Update. Bulletin of the Seismological Society of America 102: 1514-1542.

Wang X, Mountjoy JJ, Power WL, Lane EM, Mueller C 2016. Revealing the Failure Process of a Submarine Landslide near Cook Strait and Its Associated Tsunami. In: Lamarche G, Mountjoy JJ, Bull S, Hubble T, Krastel S, Lane E, Micallef A, Moscardelli L, Mueller C, Pecher I, Woelz S ed. Submarine Mass Movements and Their Consequences. 7th International Sympusium. 41.

Advances in Natural and Technological Hazards Research. Pp.

Wang X, Power WL 2011. COMCOT: a tsunami generation propagation and run-up model. GNS Science Report 2011/43 129p p.

Wilcox S, Notman P, Mountjoy J 2016. Lake Tekapo Survey.

List of Figures

Figure 1—Lake Tekapo mapping 5
Figure 2—Tsunami modelling results from landslide scenarios. 8
Figure 3—Tsunami modelling for Scenario S05. 9
Figure 4—Spatial distribution of modelled maximum tsunami heights in Lake Tekapo. 9
Figure 5—Spatial distribution of modelled maximum tsunami heights along the coasts of Lake Tekapo 10
Figure 6—Seismic profile in the central lake basin and three key regional horizons. 11
Figure 7—Conditional probability of landslide volume exceedance 13
Figure 8—Magnitude-frequency relationship for failures of the Cass Delta 13
Figure 9—An example of an estimated tsunami hazard curve 15

List of Tables

Table 1—Summary of modelled landslide scenarios. 7
Table 2—MTDs recognised in seismic and correlated with the failure of Cass Delta. 12
Table 3—Probability results for failure of Cass Delta. 12

Acknowledgements

The project team are Joshu Mountjoy and William Power (co-PI's); Xiaoming Wang (modelling lead), Susi Woelz (data acquisition and processing lead), Sean Fitzsimons, Peter Gerring, Jamie Howarth, Alan Orpin, Peter Notman and Steve Wilcox.

We are grateful to ECAN for supporting this work, particularly Helen Jack and Marion Schoenfeld. Particular thanks to the NIWA and University of Otago survey teams who put in an exceptional effort to collect the field data in challenging conditions, and to the NIWA Tekapo team for assistance and accommodation.

This report has been peer-reviewed by Emily Lane (NIWA Christchurch).